Title
Oblique nonlinear interaction of internal solitary-like waves in the Andaman Sea

Journal
International Symposium on Stratified Flows, 1(1)

Authors
Shimizu, Kenji
Nakamaya, Keisuke

Publication Date
2016-09-01

Oblique nonlinear interaction of internal solitary-like waves in the Andaman Sea

Kenji Shimizu
Formerly at CSIRO Oceans and Atmosphere
kenji.shimizu.rc@gmail.com

Keisuke Nakayama
Kobe University
nakayama@phoenix.kobe-u.ac.jp

Abstract

Oblique nonlinear interaction of two incident solitary waves, or soliton resonance, is important because it can produce a third solitary wave that has an amplitude up to 4 times the incident wave amplitude. Although this process is well studied for surface waves and in other fields of physics such as plasma, it has not been well studied for internal solitary-like waves (ISWs) in the ocean. In this study, we investigate oblique nonlinear interaction of ISWs in the Andaman Sea using three-dimensional MITgcm simulations. Our simulations demonstrate the occurrence of the oblique nonlinear interaction at several locations in the Andaman Sea. In the most prominent case, cylindrically spreading incident ISWs with less than 20 m amplitude produce an ISW of more than 70 m amplitude within ≈6 h. The modeled interaction is consistent with the Miles theory modified for incident waves with unequal amplitudes.

1. Introduction

Internal solitary-like waves (ISWs) are nonlinear and non-hydrostatic internal waves with wavelengths and periods of the order of 1 km and 10 min in the ocean. For surface waves and in other fields of physics such as plasma, it has been shown that oblique nonlinear interaction (or soliton resonance) of solitary waves with an equal amplitude can produce a third solitary wave that has an amplitude up to 4 times the incident wave amplitude. If the incident angle is smaller than a critical angle, the third wave is called a Mach stem. However, such a process is not well studied for internal waves in the ocean, probably because of difficulties for underwater measurements with both high horizontal and temporal resolution and because of high computational demand for realistic three-dimensional (3-D) numerical simulations. In this paper, we demonstrate the occurrence of the oblique ISW interaction under realistic conditions in the Andaman Sea using 3-D MITgcm simulations, and compare the results against the theory by Miles (1977) modified for unequal incident-wave amplitudes.

2. Methods

2.1. Theory for oblique interaction of solitary waves

Miles (1977) developed a theory for oblique nonlinear interaction of solitary waves. The theory assumes interaction of two infinitely long, straight solitary waves of an equal amplitude at an asymptotic state. For an incident angle smaller than a critical angle, the problem is unsteady even from a frame of reference moving with the incident solitary waves; however, it reaches an asymptotic state in which the Mach stem amplitude remains the same and the length grows linearly with time. The Miles theory has been corrected and then modified based on experimental results (e.g., Kodama 2010; Yeh et al. 2010; Li et al. 2011).

Oblique interaction of solitary waves with unequal amplitudes has been studied using the perturbation method by Johnson (1982) and Soomere (2004); however, more general solution is now available from mathematical studies (e.g., Kodama 2010). The general solution allows us to extend the Miles theory to unequal incident-wave amplitudes. The details will be presented elsewhere, but an important parameter is the modified Miles interaction parameter:

$$\kappa = \frac{\tan\Psi}{\sqrt{2\alpha\eta_m / c}\cos\Psi}, \tag{1}$$

where Ψ is half the smaller angle made by two incident solitary waves, c is the celerity, α is the quadratic nonlinear steepening parameter in the Korteweg-de Vries (KdV) equation., and

$$\sqrt{\eta_m} = \left(\sqrt{\eta_1} + \sqrt{\eta_2}\right)/2\,. \tag{2}$$

Here, η_1 and η_2 are the incident solitary-wave amplitudes. The critical angle corresponds to $\kappa = 1$. A Mach stem develops when $\kappa < 1$ except when κ is very small. It is also convenient to introduce the amplification factor:

$$a_s \equiv \frac{\eta_s}{\eta_m}, \tag{3}$$

where η_s is the amplitude of the third wave produced by the oblique interaction. Note that $a_s > 2$ indicates nonlinear amplification of solitary wave amplitude because $a_s \approx 2$ for large incident angles. Amplitifcation factor a_s can be as large as 4 when $\kappa = 1$.

The above theory can be applied to ISWs by calculating η_1, η_2, η_s, c and α using vertical modes (e.g., Holloway 1999). We consider only the 1st baroclinic mode. Its vertical structure is normalized by its maximum value, so that the amplitudes η_1, η_2, and η_s correspond to the maximum particle displacements within the water column.

As done in plasma physics, the above theory based on straight incident solitary waves can be applied to cylindrically spreading solitary waves assuming large radius of curvature compared to the wavelength (e.g., see Tsukabayashi and Nakamura 1981; Kako and Yajima 1982). In this case, the problem does not reach an asymptotic state, as geometrical spreading of the incident waves decreases the incident wave amplitudes with time.

2.2. MITgcm simulations

We use MITgcm (Marshall et al. 1997) for 3-D ISW modeling. Our model configuration takes into account nonhydrostatic effects, realistic bathymetry represented by the partial cell scheme (Adcroft et al. 1997), and free surface to allow barotropic tides. We run the model with and without Coriolis effects, and the non-rotating case is presented in this paper.

Our model grid is a plaid grid on the spherical coordinates covering the whole Andaman Sea (slightly larger than the area in Figure 1a). The horizontal resolution is 0.0025º (≈270 m) in the region of interest but becomes gradually coarser near the boundaries. The 0.0025º resolution is typically 1/4 of the minimum horizontal grid resolution necessary for resolving physical wave dispersion (Vitousek and Fringer 2011). The vertical grid resolution is 15 m near the surface and increases with depth. The number of grid points is 1800×2000×45.

We use the following input data. Bathymetry is taken from SRTM15_PLUS (updated from Becker et al. 2009). Spatially uniform initial stratification is taken from the 2013 version of World Ocean Atlas (WOA13; Locarnini et al. 2013a,b). The model boundaries are forced by horizontally varying but vertically uniform velocities from M_2 tide in TPXO8-atlas (updated from Egbert and Erofeeva 2002) and temperature and salinity from WOA13 (horizontally and temporally constant). Note that all the internal waves are produced within the model domain. Sponge zones with increased horizontal viscosity are used to dampen outgoing internal waves.

2.3. Analysis of model output

We analyze half hourly 3-D model outputs. To compare the model outputs with the modified Miles theory, we calculate the ISW amplitudes first by fitting the 1st baroclinic mode to the modeled vertical velocity, and then by relating the modal vertical velocity to the vertical displacement amplitude of ISWs using the KdV soliton solution. Since we include realistic bathymetry, the mode fitting is done using the 1st baroclinic mode calculated at each grid point assuming locally flat bottom (Shimizu 2011). Averaging along the troughs is used to calculate the mean amplitudes of incident waves and the third wave produced by the oblique interaction. The troughs are found as the location where the vertical velocity is equal to the mean of the minimum vertical velocity on the forward face and the maximum vertical

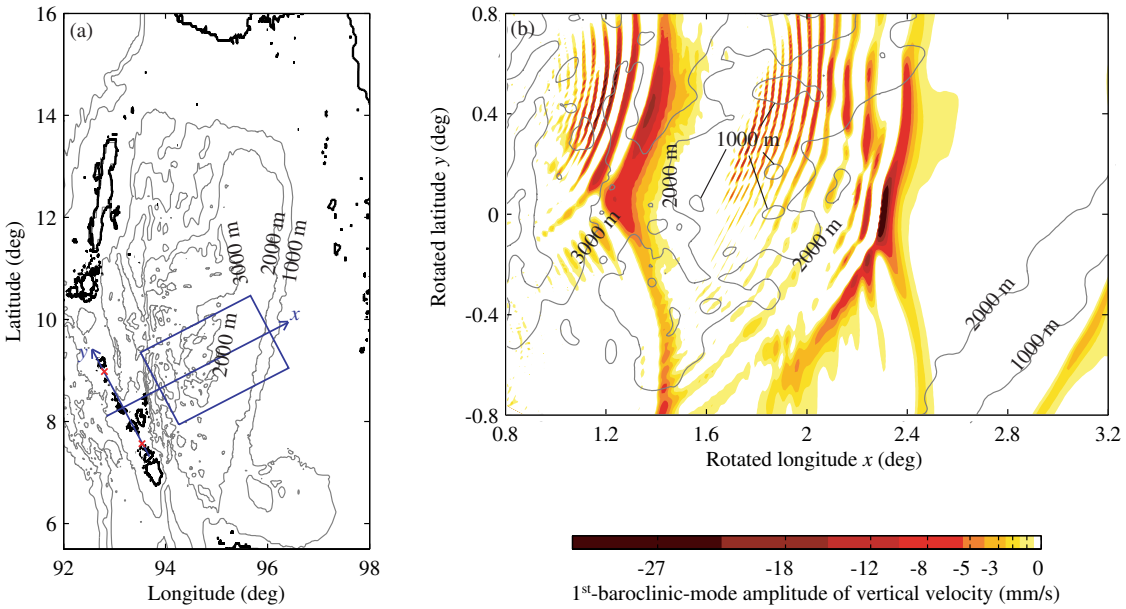

Figure 1: Model domain and snapshot of model output. (a) Approximate model domain and bathymetry, and (b) 1st-baroclinic-mode amplitude of vertical velocity within the rotated rectangle in (a). Rotated coordinates (x, y) in (a) is used to analyze model output. Approximate origins of interacting ISW packets, shown by red crosses, are located at (x, y) = (0, 0.8) and (0, -0.8). Note that only negative velocity is shown and that the color scale is nonlinear in (b).

velocity on the back face. Incident angles are calculated by fitting quadratic and linear function to the troughs of two incident waves and the third wave produced by the oblique interaction, respectively.

3. Results

Our modeling successfully produced the oblique nonlinear interaction at several locations in the Andaman Sea under realistic conditions both with and without Coriolis effects. In this paper, we focus on the most prominent interaction around (95ºE, 9ºN) in the non-rotating case (Figure 1b). A third ISW was produced by the leading ISWs of two cylindrically spreading ISW packets, originating from different sills around the Nicobar Islands. For convenience in analyzing the interaction, we introduced rotated spherical coordinates (x, y) as in Figure 1a; the approximate origins of two ISW packets are located at y = -0.8° and 0.8°. Then, we located the troughs of the leading and third ISWs and calculated the ISW amplitudes, as explained earlier (Figure 2). The amplitude of the third wave increased from less than 20 m to more than 70 m, and the length increased to ≈30 km within ≈6 h. After reaching the peak, the amplitude decreased due to cylindrical spreading. The amplitude of the southern incident ISW decreased with time as expected from cylindrical spreading. However, the amplitude of the northern incident ISW showed initial increase and subsequent decrease. One of the reasons

for the increase is that the northern incident ISW was affected by the growth of the third wave.

For comparison with the Miles theory modified for incident waves with unequal amplitudes, we calculated the interaction parameter κ and the amplification factor a_s from the model outputs. Note that, unlike the idealized theoretical setting, there was lateral variation in the ISW amplitudes as well as the curvature of the troughs (Figure 2). We used lateral mean amplitudes and incident angle $\Psi = (\Psi_1+\Psi_2)/2$, where Ψ_1 and Ψ_2 are defined in Figure 2a. For this reason, the computed κ and a_s should be seen as approximate values when compared against the theory. The interaction parameter κ was ≈1.0 in the first 4 h from the beginning of the third wave growth, while a_s increased from 2.2 to 3.2 (Table 1). Then, κ gradually increased to 1.3 while a_s reached a plateau at about 3.7. Since $\kappa \approx 1.0$ in the initial stage, it was not clear whether the third wave was a Mach stem or not. The increase of a_s under nearly constant κ was due to transitional response, as seen in the oblique interaction of cylindrically or spherically spreading solitary waves in plasma (Kaup 1981). The peak value of a_s was smaller than the theoretical peak value of 4 probably because we used mean amplitudes to calculate a_s.

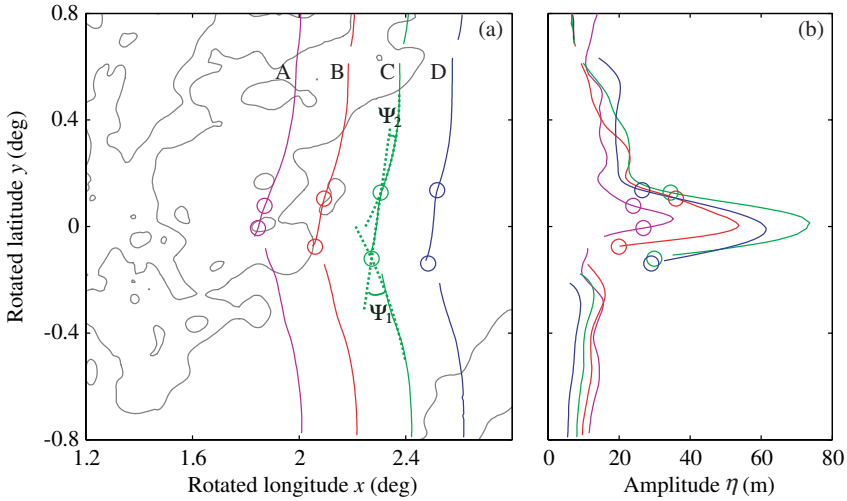

Figure 2: Characteristics of the leading ISWs in two ISW packets and the third wave produced by the oblique interaction. (a) Location of ISW troughs at 2.5 h interval, and (b) the corresponding amplitudes along the troughs. Circles show approximate boundaries between incident waves and the third wave, found as the intersections between the curves fitted to the troughs (see green dashed lines in (a)).

Table 1: Characteristics of the incident waves and the third wave produced by the oblique interaction, and the associated resonance parameters. A, B, C, and D corresponds to the times in Figure 2a.

	η_1 (m)	η_2 (m)	η_m (m)	η_s (m)	Ψ (deg)	κ (-)	a_s (-)
A	14	16	15	33	23	1.0	2.2
B	13	21	16	47	22	1.0	2.9
C	10	22	16	58	23	1.3	3.7
D	7	19	12	48	23	1.3	3.8

4. Conclusions

Our 3-D MITgcm simulations have demonstrated that the oblique nonlinear interaction of ISWs does occur under realistic conditions in the ocean. In the most prominent case, the amplification factor of ISW amplitude a_s increased to close to 4 while the Mile interaction parameter κ was $\approx$1, consistent with the Miles theory modified for incident solitary waves with unequal amplitudes.

Acknowledgements

We thank CSIRO and RPS MetOcean Pty Ltd. (Perth, Australia) for providing computational resources for this study.

References

Adcroft, A., C. Hill, and Marshall, J. (1997). Representation of topography by shaved cells in a height coordinate ocean model. *Mon. Wea. Rev.*, 125:2293–2315.

Becker, J. J., Sandwell, D. T., Smith, W. H. F., Braud, J., Binder, B., Depner, J. , Fabre, D., Factor, J., Ingalls, S., Kim, S-H., Ladner, R., Marks, K., Nelson, S., Pharaoh, A., Trimmer, R., Von Rosenberg, J., Wallace, G., and Weatherall, P. (2009). Global Bathymetry and Elevation Data at 30 Arc Seconds Resolution: SRTM30_PLUS. *Marine Geodesy*, 32:355–371.

Egbert, G. D., and Erofeeva, S. Y. (2002). Inverse modeling of barotropic ocean tides. *J. Atmos. Oceanic Tech.*, 19:183–204.

Holloway, P. E., Pelinovsky, E., and Talipova, T. (1999). A generalized Korteweg-de Vries equation model of internal tide transformation in the coastal zone. *J. Geophys. Res.*, 104:18333–18350.

Johnson, R.S. (1982). On the oblique interaction of a large and a small solitary wave. *J. Fluid Mech.*, 120:49–70.

Kako, J. and Yajima, N. (1982). Interaction of ion-acoustic solutions in multi-dimensional space II. *J. Phys. Soc. Japan*, 49:311–322.

Kaup, D.J. (1981). Nonlinear resonances and colliding spherical ion-acoustic solitons. *Physica*, 2D:389–394.

Kodama, Y. (2010). KP solitons in shallow water. *J. Phys. A: Math. Theor.*, 43:434004, doi:10.1088/1751-8113/43/43/434004.

Li, W., Yeh, H., and Kodama, Y. (2011). On the Mach reflection of a solitary wave: revisited. *J. Fluid Mech.*, 672:326–357.

Locarnini, R.A. and coauthors. (2013a). World Ocean Atlas 2013, volume 1: Temperature, *In* S. Levitus (Ed), NOAA Atlas NESDIS 73.

Locarnini, R.A. and coauthors. (2013b). World Ocean Atlas 2013, volume 2: Salinity, *In* S. Levitus (Ed), NOAA Atlas NESDIS 73.

Marshall, J., Adcroft, A., Hill, C., Perelman, L., and Heisey, C. (1997). A finite-volume, incompressible Navier-Stokes model for studies of the ocean on parallel computers. *J. Geophys. Res.*, 102:5753–5766.

Miles, J. W. (1977). Resonantly interacting solitary waves. *J. Fluid Mech.*, 79:171–179.

Shimizu, K. (2011). A theory of vertical modes in multilayer stratified fluids. *J. Phys. Oceanogr.*, 41:1694–1707.

Soomere, T. (2004). Interaction of Kadmotsev-Petviashvili solitons with unequal amplitudes. *Phys. Lett. A*, 332:74–81.

Tsukabayashi, I, and Nakamura, Y. (1981). Resonant interaction of cylindrical ion-acoustic solitons. *Phys. Lett.*, 85:151–154.

Vitousek, S., and Fringer, O. B. (2011). Physical vs. numerical dispersion in nonhydrostatic ocean modeling. *Ocean Modelling*, 40:72–86.

Yeh, H., Li, W., and Kodama, Y. (2010). Mach reflection and KP solitons in shallow water. *Eur. Phys. J. Special Topics*, 185:97–111.